Article:

Aurachman, R. orcid.org/0000-0001-6093-2190 and Punzo, G. orcid.org/0000-0003-4246-9045 (2025) Strategy diffusion and conformity in evolutionary dynamics on general networks. IEEE Control Systems Letters, 8. pp. 3398-3403. ISSN 2475-1456

https://doi.org/10.1109/lcsys.2025.3535301

Strategy Diffusion and Conformity in Evolutionary Dynamics on General Networks

Rio Aurachman[1] and Giuliano Punzo[2]

***Abstract*— Networks of social interactions can drive the dynamics of socio-technical systems. In groups, where strategic decisions are shaped by the tension between cooperation and defection, the replicator equation serves as a valuable tool underpinning the modelling of evolutionary dynamics of strategies.**

In this work, we integrate the replicator dynamics with an SI (Susceptible-Infected) model for information diffusion in general networks. Considering also conformity, we model the evolution of cooperation in a public good game. The trajectories of the resulting dynamical systems converge to consensus about an internal point solution in the snowdrift setting and boundary solutions of full cooperation or full defection in social dilemmas, asymmetric games and stag hunt settings. Through the application of the Lyapunov stability theorem, we establish the stability of the internal equilibrium point. We then examine the basin of attraction obtaining the conditions leading to full cooperation.

This work is relevant for the study of social dynamics in groups where strategic interactions are mediated by conformity.

***Index Terms*— Networks, Cooperation, Replicator, Diffusion ModelNetworks, Cooperation, Replicator, Diffusion Model**

I. Introduction

In social and biological systems, it is not uncommon to witness the renounce to selfish benefits for the common good [1]. In general, defecting and selfishly prioritising own reward is the normal course of action. Altruistic behaviours often imply costly choices. Comprehending the phenomenon of cooperative behaviour in human societies has been identified as one of the significant scientific issues of the 21st century, in particular when linked to environment and social factors [2]. It is moreover clear that individuals behave differently in isolations and groups, where networks of social ties can be considered [3] [4].

Diffusion processes, learning and games have been previously combined to understand spreading dynamics among individuals [5]. Diffusion on the general network is well understood, in particular in relation to epidemics, rumours and misinformation spread [6] [7].

For the spreading of cooperative behaviours in networks, the use of replicator dynamics is prevalent, where players replicate strategies adopted by more successful individuals, who gain more from "playing the game" [8].

It can be argued, however, that bounded rationality and non-complete information about strategies and their outcomes may prevent the spreading of winning strategy. In fact, when players interact each with a different subset of other players, the best strategy for one may be suboptimal for others. The different strategy outcomes, as well as the information players receive about them, are related to the network topology defining each player's neighbourhood. The interplay between the knowledge of the perceived best payoff and the reward from the strategy being played becomes the motivation for creating a model that combines replicator and information diffusion. This has not been explored to date to the best of our knowledge.

By combining games, information diffusion, conformity, and network setting, our work shed light on the role that these dynamics and structure have on the outcome of the repeated games.

Moving beyond the restrictions to networks with specific topologies or degree distributions [9], our model considers a general network. Every player interacts with a subset of the population and, as in the classical replicator dynamics, if a strategy yields a payout that is above the average of said subset, that strategy will be selected by more players [10].

The model we propose takes the typical structure of the network susceptible-infected (SI) diffusion model, which is chosen to govern the spreading of information about the best strategy to adopt. As different from the traditional SI models, here we consider a non constant infection rate which is determined by the pay-off matrix of the public good game, which in turn evolves with replicator dynamics.

In addition, our model also considers a conformity mechanism between player. It is believed that rational thinking is not the only factor of dynamics of strategy As shown in behavioural experiments, individuals trade off the rewards they would get from an optimal strategy, for more popular choices, to reduce risk and fit within their community [11].

While other studies have explored mixed strategies but typically in non-networked settings or general network [12], our study combines mixed strategies, general network structures, and a conformity mechanism.

II. Model Development

We will focus on repeated public good games played on a network, where each node is a player, and edges connect players in the same game. At every repetition of the game, each player will play the public good game simultaneously with all the players they are in contact with. The network is modelled as a graph $G = (V, E)$. v_i is the $i-th$ element of the set of nodes V, i.e. $v_i \in V$. E is a set of ordered pair of nodes, also known as edges and $E \subseteq v \times v$.

The adjacency matrix $A = [a_{ij}]$ captures the connection structure between nodes. We assume that the network is

[1]Rio Aurachman is a PhD student at the University of Sheffield, United Kingdom. Since 2014, he has also served as an academic at Telkom University, Bandung, Indonesia. raurachman1@sheffield.ac.uk

[2]Giuliano Punzo is with the School of Electrical and Electronic Engineering, University of Sheffield, U.K. g.punzo@sheffield.ac.uk

undirected and strongly connected, meaning that there is a path from every node to every other node. This results in the A having entries in all rows and columns. We also define the neighbour set $H_i = \{j : (v_i, v_j) \in E\}$, which indicates the set of indices for the neighbours of i. We consider a payoff matrix

$$\begin{bmatrix} P & Q \\ R & S \end{bmatrix}, \tag{1}$$

where P, Q, R, S are constant scalar values mapping to mutual cooperation (P), mutual defection (S), the payoff for cooperating with defectors (Q) and the payoff to defect while playing with cooperators (R). A mixed strategy $x_i \in \mathcal{X} = [0, 1]$, representing the degree to which a generic node i contributes (cooperates) toward the public good. Let $x_i \in \mathcal{X}$ represents the degree of cooperation by a node and its complement $1 - x_i$ will represent the degree of defection. This means that, if player i chooses to cooperate by an amount x_i, they will receive in return

$$f_{c_i} = \frac{1}{|H_i| + 1} \left(\sum_j x_j P + \sum_j (1 - x_j) Q \right) \tag{2}$$

where the sums extend to $H_i \cup i$ as i plays the game with their neighbours. Moreover, as they defect by $1 - x_i$, they will receive an additional payoff

$$f_{d_i} = \frac{1}{|H_i| + 1} \left(\sum_j x_j R + \sum_j (1 - x_j) S \right). \tag{3}$$

The mixed strategy approach aligns well with the individual-based mean field [13], popular in the study of dynamical systems. The strategy can be interpreted as the likelihood that the node is in one of the binary states 0 (defection) or 1 (cooperation). In each round of the game, players receive rewards from their chosen strategy. As this happens, each player will review and update their strategy simultaneously.

The network Susceptible-Infected (SI) model can be used as a mechanism for the spread of cooperation. In its individual mean field formulation, the SI model can be written as

$$\dot{\mathbf{x}}(t) = \beta(I_n - diag(\mathbf{x}(t)))A\mathbf{x}(t) \tag{4}$$

where the elements of the vector $\mathbf{x}$ are the probabilities of individuals to be infected and A is the (unweighted) adjacency matrix of the connection graph among the individuals. Equation (4) features a constant and scalar infection rate β to determine the probability that an infected individual spreads a disease to a susceptible one [6]. As explained in [14], the infection rate can be modified through a mechanism inspired by the replicator dynamics.

In mean field models for fully mixed populations, the replicator dynamics is $\dot{x} = x(f_c - \bar{f})$ where x is the proportion of cooperators in the population. Moreover, $\bar{f} = x\, f_c + (1-x) f_d$ is the average payoff, $f_c = P\, x + Q(1-x)$ and $f_d = R\, x + S(1-x)$ are the payoffs for cooperation and defection that depend on the proportion of cooperators and defectors. Note that the replicator equation in its scalar form can be written as

$$\dot{x} = (f_c - f_d)(1 - x)x. \tag{5}$$

The similarity between Equations (4) and (5) becomes apparent if we take $\beta = f_c - f_d$ and consider the interactions between players happening over the network, which justifies the vector form. We can hence define the vector

$$\boldsymbol{\beta} = \mathbf{f_c} - \mathbf{f_d} = [A(\mathbf{x}(P - R) + A(\mathbb{1} - \mathbf{x})(Q - S))] \tag{6}$$

as rewards are now different for each player, with elements of the vectors $\mathbf{f_c}$ and $\mathbf{f_d}$ defined by equations (2) and (3). In our settings, each player takes part in the game, choosing whether to cooperate or defect on a continuous scale. Therefore, Equation (4) for the strategy diffusion process, and Equation (6) for the actual play of the game, involve not only H_i (the neighbours of node i) but also the node v_i itself, as previously discussed. This translates into a network with self-loop in every node and a nonzero diagonal of the adjacency matrix. In the well-known SI network model, the only stable equilibrium point is at $\mathbf{x} = \mathbb{1}$ for values of the infection rate $\beta \in \,]0, 1]$ [6]. Here, $\boldsymbol{\beta}$ dynamically takes both positive and negative values, different for each player and influenced by the game dynamics as well as the value of P, Q, R, S of the payoff matrix. This makes equilibrium points other that $\mathbf{x} = \mathbb{1}$ emerge, which can be studied analytically together with their stability. In particular, this applies for the payoff matrix associated to a *snowdrift* game, which present a rick dynamics in our setting and will be considered in section III-D.

We also introduce an imitation or conformity behaviour driving the strategy evolution together with the choice protocol driven by payoff difference. We assume that, besides updating the strategy based on the reward received in comparison to the other players, each player tends to align their strategies with closest neighbours, as experiments show [15].

We consider that both strategic updates and conformity depend on the player's neighbourhood, that is, the most successful strategy are evaluated locally. This leads us to consider the strategy weighted on the neighbours $\bar{\mathbf{x}}$ as

$$\bar{\mathbf{x}} = diag^{-1}(A\mathbb{1})A\mathbf{x} = A^*\mathbf{x}. \tag{7}$$

So the evolutionary dynamics is changed into

$$\dot{\mathbf{x}}(t) = \bar{\mathbf{x}} - \mathbf{x} + diag(\boldsymbol{\beta})\, diag(\mathbb{1} - \mathbf{x})\bar{\mathbf{x}}. \tag{8}$$

From Equations (7) and (8) we get

$$\dot{\mathbf{x}}(t) = (A^* - I)\mathbf{x} + diag(\boldsymbol{\beta})\, diag(\mathbb{1} - \mathbf{x})A^*\mathbf{x}. \tag{9}$$

Note that A^* is row-stochastic. The new player-wise variable diffusion rate then becomes

$$\boldsymbol{\beta} = A^* \left[(P - R)\mathbf{x} + (Q - S)(\mathbb{1} - \mathbf{x}) \right]). \tag{10}$$

Considering $-\mathcal{L} = A^* - I$ and

$$B(x) = diag(\boldsymbol{\beta})(\, diag(\mathbb{1} - \mathbf{x})A^*). \tag{11}$$

the evolutionary dynamics can be expressed as

$$\dot{\mathbf{x}}(t) = (-\mathcal{L} + B(\mathbf{x}))\mathbf{x}. \tag{12}$$

Equation (12) represents a dynamical system that incorporates elements of both spatial structure and strategic interactions. The Laplacian $\mathcal{L}$ captures the imitation process over the local neighbourhoods while $B(x)$ accounts for the game dynamics, which represents strategic interactions among rational entities. Overall, the model combines the interplay between the stabilizing mechanism of the Laplacian and strategic interactions in game.

III. Equilibrium points

A. General Equilibrium

The equilibrium points must satisfy

$$-diag(\boldsymbol{\beta})\, diag(\mathbb{1} - \mathbf{x})A^*\mathbf{x} = 0. \tag{13}$$

We shall now look at an equilibrium point at consensus to then prove that, under some assumptions, it is the only possible equilibrium point for the system.

At consensus, i.e. where $\mathbf{x} = span\{1\}$, we get $(A^* - I)\mathbf{x} = -\mathcal{L}\mathbf{x} = 0$ as for the Laplacian of a connected graph, the eigenvector corresponding to the 0 eigenvalue is also in $span\{1\}$. Equilibrium at consensus therefore can be achieved by $\mathbf{x} = \mathbb{1}$, $\mathbf{x} = \mathbf{0}$ or $\boldsymbol{\beta} = \mathbf{0}$.

While the $\mathbf{x} = \mathbb{1}$, $\mathbf{x} = \mathbf{0}$ are immediate to verify, the condition $\boldsymbol{\beta} = \mathbf{0}$ leads to an equilibrium point which is a function of the game setting, specifically the $P - R$ and $Q - S$ values, as shown in Equation (10). As the adjacency matrix per-multiplies the expression in Equation (10), the equilibrium point obtained for $\boldsymbol{\beta} = \mathbf{0}$ does not depend on the network structure, although it may affecting uniqueness. The variation of $P - R$ and $Q - S$ values can characterize unique game types, which we are going to focus next.

B. Equilibrium for Prisoner's dilemma Game Setting

In the Prisoner's dilemma setting where $P < R$ and $Q < S$, the only stable equilibrium point is all-defect. The current modelling does not deviate from the established literature and reaches the all-defect equilibrium or $\mathbf{x} = \mathbf{0}$ [16].

Results exists about cooperation emerging as a possible equilibrium through modifications of the Prisoner's Dilemma game [17]. However, in on our model, the conformity mechanism may prevent the spread of cooperation in spatial games and undermine cooperative clusters. Even when cooperation returns higher payoff, the conformity mechanism can force cooperating nodes to defect, leading to the eventual collapse of cooperation throughout the network.

C. Equilibrium points with asymmetric game setting

In the asymmetric game setting, where $P > R$ and $Q > S$, the only stable equilibrium point corresponds to all-cooperate as cooperation is the strictly dominant strategy, ie, it is the best strategy irrespectively of the choices of other players. This is evidenced by the fact that, the payoffs of the asymmetric game make the elements of $\dot{\mathbf{x}}$ always positive when the elements of $\mathbf{x}$ are between 0 and 1. Therefore, the cooperation for each player would monotonically increase until the equilibrium $\mathbf{x} = \mathbb{1}$ is achieved.

D. Equilibrium Points With Snowdrift Game Setting

In the snowdrift game setting, where $P < R$ and $Q > S$, the stable equilibrium will vary based on the payoff matrix value. Setting $\boldsymbol{\beta} = \mathbf{0}$ in Equation (10), we get

$$-(P - R)A^*\mathbf{x} = (Q - S)A^*(\mathbb{1} - \mathbf{x}). \tag{14}$$

Assuming that the graph does not have a singular adjacency matrix [18], premultiplying both sides by A^{*-1} and rearranging, the equilibrium point becomes

$$\mathbf{x_{eq}} = \frac{(Q - S)}{(Q - S) - (P - R)}\mathbb{1}. \tag{15}$$

In contrast to previous research that explores the snowdrift game in various settings — such as iterated games [19], spatial models [20], continuous strategies [21], and N-player interactions [22] — our model proposes a relevance novel combination: a networked N-player snowdrift game with continuous strategies. With this novel framework, our findings align with those of [17], which indicate that both the traditional snowdrift game and the continuous strategy snowdrift game maintain a mixed evolutionary stable equilibrium in well-mixed populations. Similar to the prisoner's dilemma setting, this may be related to the effects of the conformity mechanism.

E. Equilibrium for the Stag Hunt Game Setting

In the stag hunt setting where $P > R$ and $Q < S$, the stable equilibrium point depends on the setting of the network and the initial condition. Here we propose a threshold that ensures the stable spread of cooperation, as will be presented in Theorem 2.

F. The Mapping of Equilibrium

After observing all possible configurations of payoff matrix, we can map the equilibria as shown in Figure 1. The equilibrium region is divided into four quadrants: full defection (dilemmas), full cooperation (asymmetric games), a region where the equilibrium cannot be determined only by the payoff matrix but is influenced by the network structure and initial conditions (stag hunt), and a quadrant presenting a continuous range of equilibria between zero and one (snowdrift).

IV. Boundness

Consistently with the model interpretation, the evolution of the state $\mathbf{x}$ in Equation (12) should follow bounded trajectories with each coordinate (player) moving between 0 (full defection) and 1 (full cooperation). This is established in the following.

Lemma 1: The trajectories of the system of equation (12), are confined within the hypercube $[0, 1]^N$ for initial conditions within hypercube. In particular, the boundary at 0 constrains the trajectories of $\mathbf{x}$ for games with equilibrium in full cooperation or internal solutions, (snowdrift or asymmetric game with $Q > S$). Similarly, the boundary at

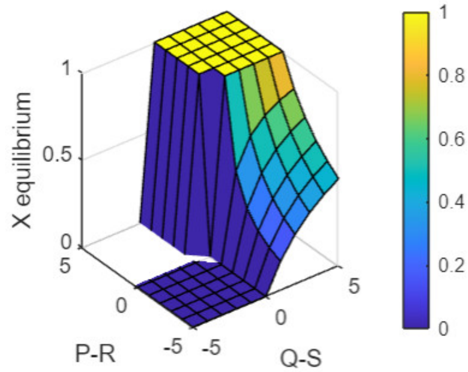

Fig. 1. Three dimensional plot showing the consensus equilibrium of the dynamical system as a function of the difference between the elements of the payoff matrix (P, Q, R, S). The regions of full defection ($\mathbf{x} = \mathbf{0}$) with $P - R < 0$ and $Q - S < 0$, full cooperation ($\mathbf{x} = \mathbb{1}$) with $P - R > 0$ and $Q - S > 0$, and the interior point corresponding to the equilibrium in ($\mathbf{0} < \mathbf{x} < \mathbb{1}$) with $P - R < 0$ and $Q - S > 0$ are visible. The region corresponding to $P - R > 0$ and $Q - S < 0$ is not considered since in this case the equilibrium depends on the initial conditions and the network topology, and cannot be defined solely by the payoff matrix.

1 constrains the trajectories for games with equilibrium in full defection or internal solutions (snowdrift and prisoner's dilemma with $P < R$).

Proof: Consider the dynamics near the boundaries of the hypercube and define $\mathbf{F}(\mathbf{x})$ such that $\dot{\mathbf{x}} = \mathbf{F}(\mathbf{x})$. The state close to the boundary at $\mathbf{0}$ can be written as $\mathbf{x} = \mathbf{0} + \mathbb{1}\epsilon$, where ϵ is an arbitrarily small number.

The limit value of ϵ to zero, or $\mathbf{F}(\mathbf{0}+\mathbb{1}\epsilon)$, can be calculated using L'Hospital Theorem or

$$\lim_{\mathbf{x}\to\mathbf{0}} \mathbf{F}(\mathbf{x}) = \lim_{\epsilon\to 0} \mathbf{F}(\mathbf{0}+\mathbb{1}\epsilon) = \left.\frac{\partial \mathbf{F}(\mathbf{0}+\mathbb{1}\epsilon)}{\partial \epsilon}\right|_{\epsilon=0} = (Q-S)\mathbb{1}. \tag{16}$$

Equation (16) will have a positive value if $Q > S$, which indicates that the system state will move from the $\mathbf{x} = \mathbf{0}$ towards equilibrium. This proves the boundary at $\mathbf{x} = \mathbf{0}$ for the snowdrift game, which has the equilibrium $\mathbf{x_{eq}} = \frac{(Q-S)}{(Q-S)-(P-R)}\mathbb{1}$ and the asymmetric game with the equilibrium $\mathbf{x} = \mathbb{1}$.

For the boundary at $\mathbf{x} = \mathbb{1}$ we calculate the derivation of $\mathbf{F}(\mathbb{1} - \mathbb{1}\epsilon)$ which results in

$$\lim_{\mathbf{x}\to\mathbf{1}} \mathbf{F}(\mathbf{x}) = \lim_{\epsilon\to 0} \mathbf{F}(\mathbb{1}-\mathbb{1}\epsilon) = \left.\frac{\partial \mathbf{F}(\mathbb{1}-\mathbb{1}\epsilon)}{\partial \epsilon}\right|_{\epsilon=0} = (P-R)\mathbb{1}. \tag{17}$$

Equation (17) will have a negative value if $P < R$, which indicates that the state of the system will move from $\mathbf{x} = \mathbf{1}$ to equilibrium. This proves the boundary at $\mathbf{x} = \mathbb{1}$ for the snowdrift game, which has the equilibrium $\mathbf{x_{eq}} = \frac{(Q-S)}{(Q-S)-(P-R)}\mathbb{1}$ and the prisoner dilemma with the equilibrium $\mathbf{x} = \mathbf{0}$. ■

V. Stability

Theorem 1: The dynamical system in Equation (12) is globally asymptotically stable (GAS) at the equilibrium point $\mathbf{x_{eq}} = \frac{(Q-S)}{(Q-S)-(P-R)}\mathbb{1}$ if $Q - S > P - R$.

Proof: To prove that the equilibrium $\mathbf{x_{eq}} = \frac{(Q-S)}{(R-P)+(Q-S)}\mathbb{1}$ is GAS, consider the Lyapunov function

$$V = \frac{1}{2}(\mathbf{x} - \mathbf{x}_{eq})^T(\mathbf{x} - \mathbf{x}_{eq}), \tag{18}$$

which is always positive and zero when $\mathbf{x} = \mathbf{x}_{eq}$. Moreover $V(\mathbf{x}-\mathbf{x}_{eq})$ is radially unbounded. The time derivative yields

$$\dot{V} = (\mathbf{x} - \mathbf{x}_{eq})^T\dot{\mathbf{x}}. \tag{19}$$

For simplicity, by defining $g \triangleq \mathbf{x} - \mathbf{x}_{eq}$, we can write $\dot{V} = g^T\dot{\mathbf{x}}$. It follows that $\boldsymbol{\beta} = A^*(-\mathbf{g}((Q - S) - (P - R)))$, $l = Q - S$ and $k = P - R$, so

$$\boldsymbol{\beta} = (k - l)A^*\mathbf{g}. \tag{20}$$

The Lyapunov function then becomes

$$\dot{V} = \mathbf{g}^T((A^* - I)\mathbf{x} + diag(\boldsymbol{\beta})\, diag(\mathbb{1} - \mathbf{x})A^*\mathbf{x}).$$

As

$$diag(\boldsymbol{\beta})A^*\mathbf{x} = (k - l)diag(A^*\mathbf{g})A^*\mathbf{x} \tag{21}$$

and $diag(A^*\mathbf{g})A^*\mathbf{x} = diag(A^*\mathbf{x})A^*\mathbf{g}$, we can write

$$\dot{V} = \mathbf{g}^T((A^* - I)\mathbf{x} + diag(\mathbb{1} - \mathbf{x})diag(A^*\mathbf{x})\ (k - l)A^*\mathbf{g}). \tag{22}$$

This leads to

$$\dot{V} = -\mathbf{g}^T\mathcal{L}\mathbf{x} - (l - k)\mathbf{g}^T D^+\, A^*\mathbf{g},$$

where

$$D^+ = diag(\mathbb{1} - \mathbf{x})diag(A^*\mathbf{x}). \tag{23}$$

Recalling that $\mathbf{x} = \mathbf{g} + \mathbf{x}_{eq}$, we get

$$\dot{V} = -\mathbf{g}^T\mathcal{L}\mathbf{g} - (\mathbf{g}^T\mathcal{L}\mathbf{x}_{eq}) - (l - k)\mathbf{g}^T D^+\, A^*\mathbf{g}. \tag{24}$$

As $x_{eq} \in span\{1\}$, the middle term of Equation (24) is null. The first term is nonpositive as the Laplacian is positive semidefinite and D^+A^* has all nonnegative entries that, with A^* being nonsingular makes the last term is negative too. It can therefore be concluded that $\dot{V}$ is negative as long as $l > k$. ■

Corollary 1: The dynamical system in Equation (12) has globally asymptotically stable equilibrium points at $\mathbf{x} = \mathbf{0}$ and $\mathbf{x} = \mathbb{1}$ for $Q < S$, $P < R$ and $Q > S$, $P > R$ respectively.

Proof: The proof of the stability for $\mathbf{x} = \mathbf{0}$ follows directly from Theorem 1 and is omitted for brevity. In fact, both satisfy Equation (13) at consensus and the statement simply follows by considering the boundness of the dynamics, therefore can be obtained as special cases of Theorem 1. ■

While just a special case of the consensus equilibrium, this results shows the possibility of obtaining any equilibrium point in the snowdrift game, including one in pure strategies. We can now relate the initial conditions, ie the strategy at the onset of the game, with the values of the payoff matrix.

Theorem 2: The cooperation will spread throughout the network if

$$k > sup^{\mathbb{1}}_{\mathbf{x}=\mathbf{x}_0} - \frac{(\mathbf{x} - \mathbb{1})^T(-\mathcal{L}\mathbf{x} + l\ diag(\mathbb{1} - A^*\mathbf{x})\mathbf{d}^+}{(\mathbf{x} - \mathbb{1})^T diag(A^*\mathbf{x})\mathbf{d}^+}, \tag{25}$$

Where $\mathbf{d}^+ = diag(\mathbb{1} - \mathbf{x})A^*\mathbf{x}$

Proof: To prove the asymptotic stability of the equilibrium point $\mathbf{x} = \mathbb{1}$, we propose the following Lyapunov function

$$V = \frac{1}{2}(\mathbf{x} - \mathbb{1})^T(\mathbf{x} - \mathbb{1}). \quad (26)$$

The V value is positive because squared and zero when $\mathbf{x} = \mathbb{1}$. The time derivative yields

$$\dot{V} = (\mathbf{x} - \mathbb{1})^T\dot{\mathbf{x}} \quad (27)$$

$$\dot{V} = (\mathbf{x}-\mathbb{1})^T((A^*-I)\mathbf{x}+diag(\boldsymbol{\beta})\, diag(I-\mathbf{x})A^*\mathbf{x}). \quad (28)$$

where $\boldsymbol{\beta}$ can also be written as

$$\boldsymbol{\beta} = (P - R)A^*\mathbf{x} + (Q - S)A^*(\mathbb{1} - \mathbf{x})\ . \quad (29)$$

Therefore, $\dot{V}$ can be written as

$$\dot{V} = (\mathbf{x}-\mathbb{1})^T((A^*-I)\mathbf{x}+diag(\boldsymbol{\beta})\, diag(\mathbb{1}-\mathbf{x})A^*\mathbf{x}). \quad (30)$$

Substituting for $\boldsymbol{\beta}$ and imposing $\dot{V} < 0$, we get

$$\begin{aligned} &- (P - R)(\mathbf{x} - \mathbb{1})^T diag(A^*\mathbf{x})diag(\mathbb{1} - \mathbf{x})A^*\mathbf{x} > \\ &(\mathbf{x} - \mathbb{1})^T((A^* - I)\mathbf{x} \\ &+ (Q - S)(\mathbf{x} - \mathbb{1})^T diag(\mathbb{1} - A^*\mathbf{x})diag(\mathbb{1} - \mathbf{x})A^*\mathbf{x})\ . \end{aligned} \quad (31)$$

Rearranging we get

$$k > -\frac{(\mathbf{x} - \mathbb{1})^T(-\mathcal{L}\mathbf{x} + l\ diag(\mathbb{1} - A^*\mathbf{x})\mathbf{d}^+)}{(\mathbf{x} - \mathbb{1})^T diag(A^*\mathbf{x})\mathbf{d}^+} \quad (32)$$

Finally, the theorem is proved by considering the supremum to impose all initial conditions are within the threshold. ■

We note here that our theoretical results rely on the network strong connectivity which guaranteee that expressions such as (25) return finite values.

VI. Numerical Simulation

To validate our analytical results, we perform numerical simulations by integrating Equation (12) using both real-world and artificial networks. The real-world networks include an undirected and unweighted tailor employee Network (TE) with 39 nodes and 169 edges [23], a mobile phone connection network (MP) with 1984 nodes and 31790 edges [24], and a biological macrophage network (BM) with 475 nodes and 2162 edges replicated from [9]. Additionally, we generate artificial 10-node networks, including Erdős-Rényi, regular, star, and line topologies. In all cases, we analyze the time evolution of cooperation and compare the equilibrium points obtained from MATLAB-based ordinary differential equation simulations with the corresponding analytical solutions. Our observations are summarized in Fig. 2. It can be seen that, for each simulation, the equilibrium value and its stability from the analytical results align with the simulation outcomes. Panels (a) and (b) show consistency with Theorem 1, using two different networks with random initial conditions, and snowdrift game setting. Irrespectively of the initial conditions, the simulated dynamics converge to a specific mixed-strategy equilibrium point $\mathbf{x}_{\text{eq}}$, determined by the payoff matrix (red star).

Panels (c), (e), and (f) validate Theorem 2 with the stag hunt game setting. In panel (c), using the microphage network and same randomized initial conditions, the increase of k from 1 to 2 shifts the system from a defection equilibrium to a cooperation equilibrium. Panel (f) shows how changes of the network structure will affect cooperation. While difficult to evidence from the figure, we note that, in the numerical simulations, highly connected networks diminish cooperation in the stag hunt settings, which correspond to an increase of the threshold (25).

Panel (d) in particular validates Corollary 1, demonstrating that the dominant strategy—whether cooperation or defection—converges to a stable equilibrium of all cooperation or all defection, respectively. Regardless of the variety of settings and initial conditions, the boundness claimed in Lemma 1, is always verified.

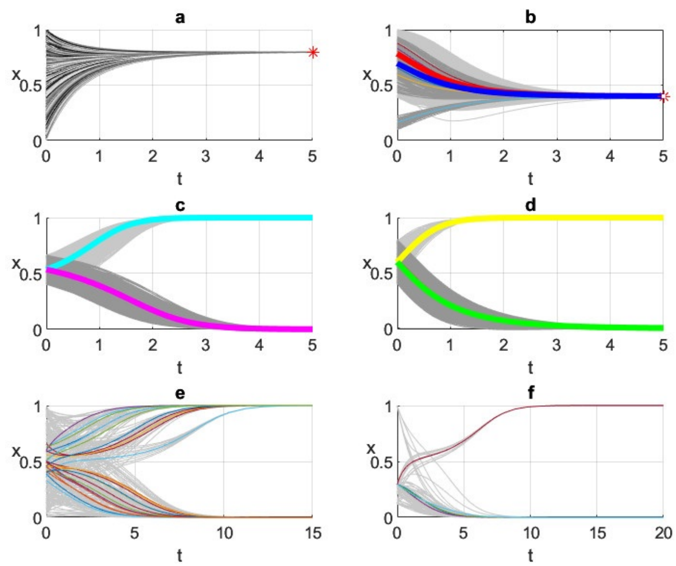

Fig. 2. Trajectory plots of the dynamical system using Tailor Employee (TE), Mobile Phone Connection (MP) and Biological Microphage (BM) networks. Thin colored lines represent the average of each set of simulations, bold colored lines represent the overall average across all sets, and gray lines represent individual node trajectories within each set. (a) Snowdrift with MP network. Red dot represent equilibrium point by analytical calculation from Theorem 1. (b) Corresponding to Theorem 1, the snowdrift game with payoff matrix $P, Q, R, S = 3, 6, 6, 4$. The light gray and thick red lines represent the BM network, while the darker gray and bold blue lines represent the TE network. (c) Corresponding to Theorem 2, the stag hunt game with the BM network and $l = -2$. The light gray and thick cyan lines represent $k = 2$, while the dark gray and thick magenta lines represent $k = 1$. (d) Corresponding to Corollary 1 and TE network, light gray and thick yellow lines represent the payoff matrix $P, Q, R, S = 5, 4, 2, 3$, and dark gray and thick green lines represent the payoff matrix $P, Q, R, S = 2, 3, 5, 4$. (e,f) The stag hunt game with $P, Q, R, S = 6, 5, 5, 6$ is simulated on 10-node artificial network, corresponding to Theorem 2. (e) Simulated star network with several random sets of initial conditions. (f) Same initial condition but different 10-node network topologies.

VII. Conclusions

This work proposes a novel dynamical system model that combines the replicator equation and the SI model on networks. The payoff matrix determines the consensus-type stable equilibrium point of the dynamical system. The state of each node represents the proportion of cooperation, coinciding with their strategy bounded between zero (total defection) and one (full cooperation). The dynamics are a combination of the consensus process and the game process.

We departed from a number of assumptions that are popular in the literature on the evolution of cooperative behaviours such as only considering pure strategies in either well-mixed populations or generic networks [10]. We propose a model that suits general networks, using mixed strategies, and inducing a conformity mechanism. This allows for understanding how initial conditions network and payoff structures affect the spread of cooperation. While the literature offers the analysis of some of these factors in isolation [25] [26], our study explores their combined effects on the emergence of stable equilibria, considering both internal solutions and boundary points. This finding is made possible by the newly integrated proposed framework.

Some limitations arise from the intrinsic consensus converging nature of the dynamics. In fact, the model leverages a diffusive dynamics that employs game mechanisms, setting it apart from the traditional framework of evolutionary game dynamics as in [4]. Results about to non-consensus stable equilibrium are available in the literature, notably in [27]. However they tend to rely heavily on numerical results and limited to specific game settings (social dilemmas in the case of [27]). Our approach does not capture the full variety of possible outcomes, which may expand when considering differences between players, in addition to different neighbour sets. This may explain the limited set of equilibria we account for. On the other hand, our approach allows for a detailed understanding of how cooperation spreads through the network at the level of individual nodes with mixed strategies, a concept that also motivates research in epidemic modelling. Overcoming of some limitations could be obtained by implementing node-based payoff matrices, where each player compete in their own version of the game. This could extend to including zealots as well.

Potential applications of this model include social systems, as demonstrated with the Tailor employee network (Figure 2(b)). Additionally, this model can serve as an approach for controlling distributed systems requiring imitation and conformity among agents, as simulated and illustrated for the mobile phone connection network (Figure 2(a)).

Finally, we note that our model is open to replacing the SI diffusion mechanism with other diffusion and opinion dynamics models. The game setting can also be extended from the public goods game to other game scenarios. Additionally, it is possible to use our results as basis to study optimal incentives to promote cooperation amongst multiple decision makers.

ACKNOWLEDGMENT

This work was funded by BPPT (Centre for Higher Education Funding) and LPDP (Indonesia Endowment Fund for Education) under the Government of Indonesia.

REFERENCES

[1] M. Perc, J. J. Jordan, D. G. Rand, Z. Wang, S. Boccaletti, and A. Szolnoki, "Statistical physics of human cooperation," 2017.
[2] E. Pennisi, "How did cooperative behavior evolve," 2005.
[3] J. Riehl, P. Ramazi, and M. Cao, "A survey on the analysis and control of evolutionary matrix games," 2018.
[4] M. A. Nowak, C. E. Tarnita, and T. Antal, "Evolutionary dynamics in structured populations," 2010.
[5] M. O. Jackson, *An overview of social networks and economic applications*, 2011, vol. 1.
[6] F. Bullo, *Lectures on Network Systems*, 2018.
[7] S. Shelke and V. Attar, "Source detection of rumor in social network – a review," 2019.
[8] P. D. Taylor and L. B. Jonker, "Evolutionary stable strategies and game dynamics," *Mathematical Biosciences*, vol. 40, 1978.
[9] S. Tan and Y. Wang, "Graphical nash equilibria and replicator dynamics on complex networks," *IEEE Transactions on Neural Networks and Learning Systems*, vol. 31, 2020.
[10] H. Ohtsuki and M. A. Nowak, "The replicator equation on graphs," *Journal of Theoretical Biology*, vol. 243, 2006.
[11] L. Zhang, C. Huang, H. Li, Q. Dai, and J. Yang, "Cooperation guided by imitation, aspiration and conformity-driven dynamics in evolutionary games," *Physica A: Statistical Mechanics and its Applications*, vol. 561, 2021.
[12] J. Y. Li, W. H. Wu, Z. Z. Li, W. X. Wang, and B. Zhang, "Data-driven evolutionary game models for the spread of fairness and cooperation in heterogeneous networks," *Frontiers in Psychiatry*, vol. 14, 2023.
[13] P. V. Mieghem, J. Omic, and R. Kooij, "Virus spread in networks," *IEEE/ACM Transactions on Networking*, vol. 17, 2009.
[14] R. Aurachman and G. Punzo, "On the relation between replicator evolutionary dynamics and diffusive models on general networks," vol. 1142 SCI, 2024.
[15] S. E. Asch, *Effects of group pressure upon the modification and distortion of judgments*, 2023.
[16] R. Axelrod and W. D. Hamilton, "The evolution of cooperation," *Science (New York, N.Y.)*, vol. 211, 1981.
[17] M. Doebeli and C. Hauert, "Models of cooperation based on the prisoner's dilemma and the snowdrift game," 2005.
[18] I. Sciriha, "A characterization of singular graphs." *ELA. The Electronic Journal of Linear Algebra [electronic only]*, vol. 16, pp. 451–462, 2007. [Online]. Available: http://eudml.org/doc/129125
[19] F. Dubois and L. A. Giraldeau, "The forager's dilemma: Food sharing and food defense as risk-sensitive foraging options," *American Naturalist*, vol. 162, 2003.
[20] T. Killingback and M. Doebeli, "Spatial evolutionary game theory: Hawks and doves revisited," *Proceedings of the Royal Society B: Biological Sciences*, vol. 263, 1996.
[21] M. Doebeli, C. Hauert, and T. Killingback, "The evolutionary origin of cooperators and defectors," *Science*, vol. 306, 2004.
[22] C. Hauert, F. Michor, M. A. Nowak, and M. Doebeli, "Synergy and discounting of cooperation in social dilemmas," *Journal of Theoretical Biology*, vol. 239, 2006.
[23] B. Kapferer, *Strategy and Transaction in an African Factory: African Workers and Indian Management in a Zambian Town*, 1972, vol. 43.
[24] J. Tang, T. Lou, J. Kleinberg, and W. Sen, "Transfer link prediction across heterogeneous social networks," *TOIS*, vol. 15, 2014.
[25] F. Parise and A. Ozdaglar, "Analysis and interventions in large network games," 2021.
[26] Z. Wang, L. Wang, A. Szolnoki, and M. Perc, "Evolutionary games on multilayer networks: a colloquium," *European Physical Journal B*, vol. 88, 2015.
[27] A. Szolnoki and X. Chen, "Competition and partnership between conformity and payoff-based imitations in social dilemmas," *New Journal of Physics*, vol. 20, 2018.